ACS Medicinal Chemistry Letters

pubs.acs.org/acsmedchemlett

Letter

Discovery of the TLR7/8 Antagonist MHV370 for Treatment of Systemic Autoimmune Diseases

Phil Alper,* Claudia Betschart, Cédric André, Thomas Boulay, Dai Cheng, Jonathan Deane, Michael Faller, Roland Feifel, Ralf Glatthar, Dong Han, Rene Hemmig, Tao Jiang, Thomas Knoepfel, Jillian Maginnis, Daniel Mutnick, Wei Pei, Giulia Ruzzante, Peter Syka, Guobao Zhang, Yi Zhang, Florence Zink, Géraldine Zipfel, Stuart Hawtin, Tobias Junt, and Pierre-Yves Michellys

Cite This: *ACS Med. Chem. Lett.* 2023, 14, 1054−1062

Read Online

ACCESS | Metrics & More | Article Recommendations | Supporting Information

ABSTRACT: Toll-like receptor (TLR) 7 and TLR8 are endosomal sensors of the innate immune system that are activated by GU-rich single stranded RNA (ssRNA). Multiple genetic and functional lines of evidence link chronic activation of TLR7/8 to the pathogenesis of systemic autoimmune diseases (sAID) such as Sjögren's syndrome (SjS) and systemic lupus erythematosus (SLE). This makes targeting TLR7/8-induced inflammation with small-molecule inhibitors an attractive approach for the treatment of patients suffering from systemic autoimmune diseases. Here, we describe how structure-based optimization of compound **2** resulted in the discovery of **34** (MHV370, (*S*)-N-(4-((5-(1,6-dimethyl-1*H*-pyrazolo[3,4-*b*]pyridin-4-yl)-3-methyl-4,5,6,7-tetrahydro-1*H*-pyrazolo[4,3-*c*]pyridin-1-yl)methyl)bicyclo[2.2.2]octan-1-yl)-morpholine-3-carboxamide). Its *in vivo* activity allows for further profiling toward clinical trials in patients with autoimmune disorders, and a Phase 2 proof of concept study of MHV370 has been initiated, testing its safety and efficacy in patients with Sjögren's syndrome and mixed connective tissue disease.

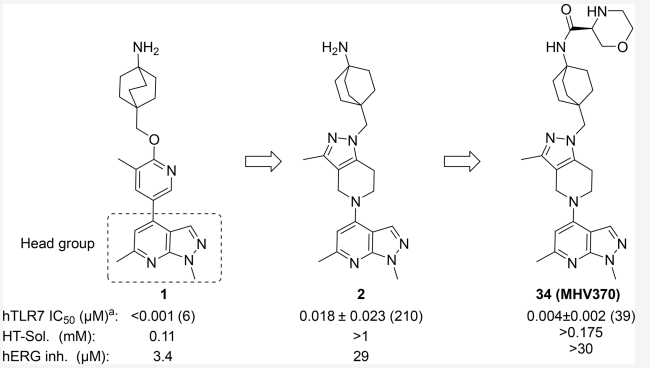

KEYWORDS: *Toll-like receptor 7, toll-like receptor 8, lupus, innate immunity, SAR*

Toll-like receptors (TLRs) are evolutionarily conserved type I transmembrane proteins of the innate immune system that recognize conserved molecular patterns (pathogen associated molecular patterns, PAMPs), which are present in proteins, lipids, and nucleic acids from pathogens. Activation of TLR pathways leads to host defense mechanisms such as secretion of inflammatory cytokines, induction of interferon pathways and activation of B cells and neutrophils.[1] The endosomal TLRs, TLR3, TLR7/8 and TLR9 recognize double stranded RNA (dsDNA), GU-rich single stranded RNA (ssRNA) and nonmethylated single stranded DNA (ssDNA), respectively. Aberrant activation of these nucleic acid sensing endosomal TLRs has been invoked as a potential driver of autoimmune diseases such as systemic lupus erythematosus (SLE) and Sjögren's syndrome (SjS).[2,3]

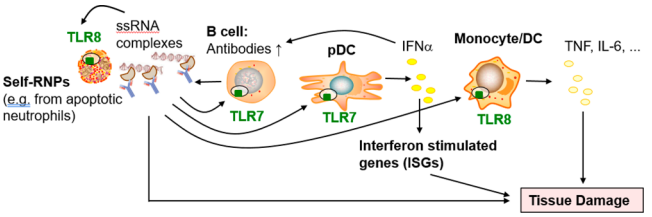

Figure 1. Role of TLR7 and TLR8 in the pathology of SLE and related chronic inflammatory diseases. ssRNA complexes are immune complexes of RNPs and autoantibodies or complexes of ssRNA with amphiphilic peptides.

Genetic and functional evidence suggests chronic hyperactivation of TLR7/8 by endogenous ssRNA as a driver of several systemic autoimmune diseases. For example, TLR7 gain-of-function mutations were found in children suffering from severe autoimmunity, and expression of one such mutant in mice causes lethal lupus-like disease,[4] as does overexpression of TLR7[5] or human TLR8.[6]

Increased activation of TLR7 and TLR8 drives multiple cellular mechanisms of systemic autoimmune diseases. For

Received: April 13, 2023
Accepted: June 30, 2023
Published: July 31, 2023

https://doi.org/10.1021/acsmedchemlett.3c00136
ACS Med. Chem. Lett. 2023, 14, 1054−1062

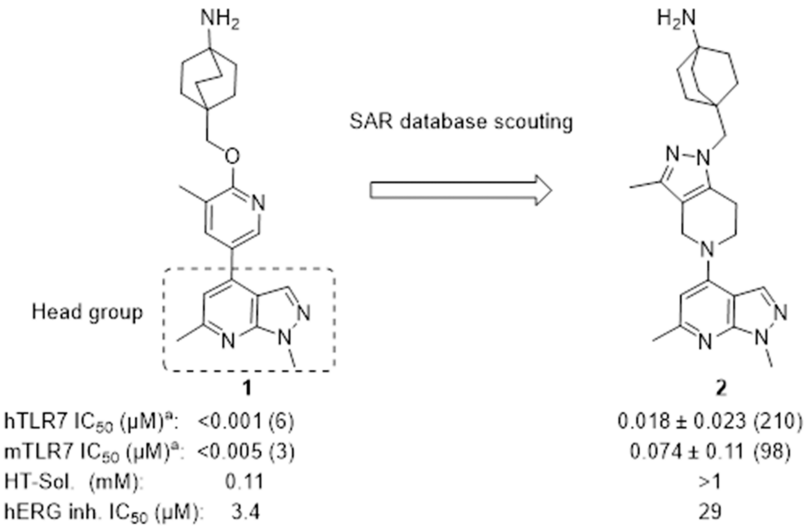

Figure 2. Discovery of compound **2** by SAR database scouting TLR7 cellular assays in human PBMCs and mouse splenocytes; details in the Supporting Information. [a]IC_{50} ± SD, numbers in parentheses denote the number of independent experiments.

Scheme 1. Synthesis of Compound 2[a]

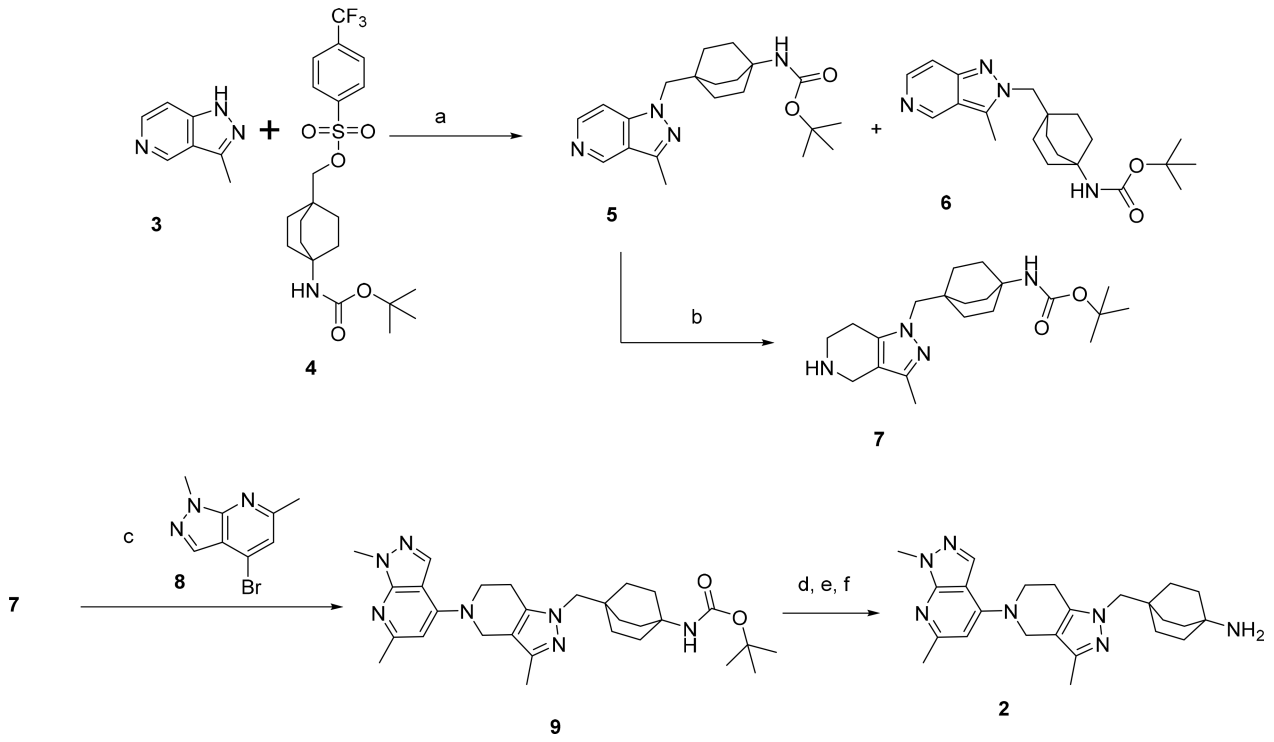

[a]Reagents and conditions. a. Cs_2CO_3, DMSO, 120°C, 18 h. b. H-cube. c. Pd_2dba_3, RuPhos, Cs_2CO_3, THF, 80°C, 18 h. d. 4 N HCl/dioxane, MeOH, RT, 1h. e. Crystallization in IPA. f. Ambersep900OH, MeOH, rt, 1 h.

example, RNA-containing immune complexes (ICs) between autoantibodies of patients and ribonucleoproteins (RNPs) drive secretion of type I interferon (IFNs) from plasmacytoid dendritic cells (pDCs) in a TLR7-dependent manner,[7] and IFNs[8] along with an elevated IFN stimulated gene signature[9] are characteristic features of SLE patients. Neutrophils get activated via TLR8[10] autoreactive B cells internalize RNA-containing autoantigens for TLR7 activation[11] and complexed RNA-containing autoantigens are engulfed by monocytes/DCs for activation of TLR8.[12] Together, enhanced activation of autoreactive B cells, pDCs and monocytes/DCs via TLR7/8 increases the secretion of antineuclear antibodies (ANAs) and sustains a self-perpetuating feedback loop of inflammation and tissue damage (Figure 1).

Consequently, TLR7/8 antagonists could serve to break this vicious loop in patients and developing small-molecule inhibitors is an attractive approach for the treatment of such autoimmune indications[13−15]

We recently described a series of potent TLR7/8 antagonists discovered in a phenotypic screen.[13] This effort was focused around modulating the amine moiety to address the liabilities of the piperazine group in the primary hit and on potency

https://doi.org/10.1021/acsmedchemlett.3c00136
ACS Med. Chem. Lett. 2023, 14, 1054−1062

Table 1. ADME/Physicochemical and Mouse PK Profiles of Compound 2

ADME profile of **2**		mouse PK profile of **2**			
CYP 3A4 (μM)	>50[a]	IV dosing (3 mg/kg)		PO dosing (20 mg/kg)	
h, m, r Met CL (μL/min/mg)	19, 15, 36	AUC (h[a]nM)	5005	AUC (h·nM)	1146
Caco2 (A-B/B-A); ratio	2.1/15.7; 7.5	CL (mL/min/kg)	24	Cmax (nM)	321
LogPAMPA (cm/s)	−5.1	Cmax (nM)	321	Clast; Tlast (nM; h)	35; 7
CYP 3A4 TDI (K_i/Kinact)	0.002	Vss (L/kg)	4.1	MRT (h)	2.9
PXR (CYP induction)	7.9%[b]	T1/2 (h)	2.1	%F	4

[a]Inhibition of CYP 2D9 and CYP 2D6 with IC_{50} of >25 μM. [b]Rifampicin was used as standard (set at 100%). IV and PO formulation: 2.9 mg/mL in PEG300/D5W, 3:1; solution.

optimization through identification of the most adequate "head group" (4-substituted 1,6-dimethyl-1*H*-pyrazolo[3,4-*b*]-pyridine) moiety to optimize potency; compound **1**, Figure 2. Here we expand on our SAR optimization of a subseries of **1** that allowed us to identify the clinical candidate compound **34** ((*S*)-*N*-(4-((5-(1,6-dimethyl-1*H*-pyrazolo[3,4-*b*]pyridin-4-yl)-3-methyl-4,5,6,7-tetrahydro-1*H*-pyrazolo[4,3-*c*]pyridin-1-yl)-methyl)bicyclo[2.2.2]octan-1-yl)morpholine-3-carboxamide, MHV370),

Although **1** (Figure 2) was a potent TLR7 antagonist, it was not suitable as a drug candidate due to its physicochemical properties (low solubility) and hERG inhibition. These properties were evident across the entire series and as a consequence impossible to improve by staying within the current compound configuration (i.e., aromatic or hetero-aromatic ring appended to the bicyclic 1,6-dimethyl-1*H*-pyrazolo[3,4-*b*]pyridine moiety). For this reason, we made selected changes to the scaffold focusing on decreasing sp^2 character. This resulted in compound **2**, which had adequate potency on TLR7 in human PBMCs (IC_{50} of 0.018 ± 0.023 μM, n = 210) and mouse splenocytes (IC_{50} of 0.074 ± 0.11 μM, n = 98) and displayed an improved solubility and hERG inhibition profile (IC_{50}: 29 μM), as shown in Figure 2.

The synthesis of **2** is depicted in Scheme 1. Alkylation of **3** with **4** using Cs_2CO_3 in DMSO at 120 °C for 18 h afforded an easily separable mixture of **5** and **6**. Hydrogenation (H cube) of **5** afforded **7** quantitatively. Buchwald coupling of **7** and **8** in the presence of Pd_2dba_3, RuPhos, and Cs_2CO_3 in THF at 80 °C afforded the Boc derivative **9**. Boc deprotection (4 N HCl/dioxane) followed by recrystallization in IPA and trituration in a slurry of Ambersep9000OH in MeOH at rt afforded **2** in 90% yield.

When profiled for its ADME properties, **2** showed poor permeability (log PAMPA = −5.1) associated with a strong efflux in the Caco2 assay (ratio A-B/B-A = 15.2). When **2** was tested for its PK properties in mice at doses of 5 mg/kg IV and 20 mg/kg PO as a solution (formulation PEG300/D5W, 3:1), it displayed a moderate clearance (24 mL/min/kg), high Vss (4.1 L/kg), short MRT (2.9 h), and low oral bioavailability of 4%, consistent with the observed permeability and efflux data. The data collected on **2** are displayed in Table 1.

We hypothesized that the free amine appended to the octabicyclic system was responsible for the lack of permeability and therefore evaluated several amine-capping substitutions

Scheme 2. Synthetic Route of Alkyl-Substituted Amines[a]

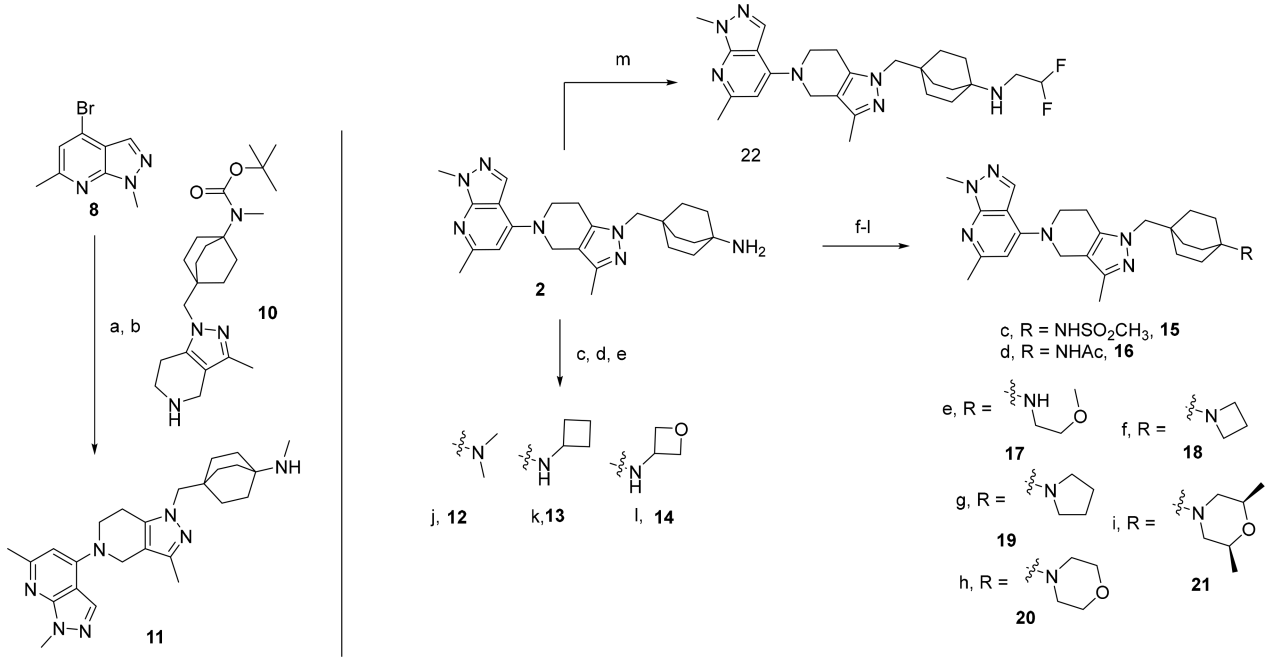

[a]Reagents and conditions: a. Pd_2dba_3, Cs_2CO_3, RuPhos, dioxane, **10**, reflux 18 h. b. HCl-dioxane, RT. c. Paraformaldehyde, DIEPA, $NaBH_3CN$, THF/MeOH, RT. d. Cyclobutanone, $NaBH_3CN$, AcOH, MeOH, RT to 75°C. e. Oxetan-3-one, $NaBH_3(OAc)_3$, DCE, AcOH, RT. f, AcCl or MsCl, DIPEA, DCM, 0°C to RT. g. 1-Bromo-2-methoxyethane, K_2CO_3, IPA, reflux. h/k. Corresponding dialkyl bromide, K_2CO_3, EtOH, 120°C, MW irradiation, 30 min. l. (*S*)-1-(4-Methylbenzenesulfonate)-2-(((*R*)-1-(4-methylbenzenesulfonate)-2-yl)oxy)propane, DIEPA, DMA, 100°C, 18h. m. 2,2-Difluoroethyl trifluoromethanesulfonate, DIPEA, THF, reflux, ON.

https://doi.org/10.1021/acsmedchemlett.3c00136
ACS Med. Chem. Lett. 2023, 14, 1054−1062

Table 2. Profiling Data of Compounds 2, 11−22[a]

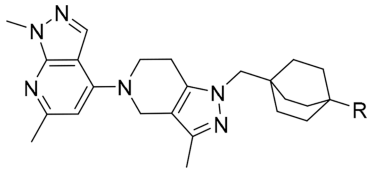

R	cmp	hTLR7	hTLR8	hTLR9	Log PAM PA	HT-Sol.	hERG	CYP3A4	TDI	Met CL (h. m. r)
NH_2	**2**	0.02±0.02 (210)	0.21±0.18 (216)	0.58±1.02 (143)	-5.1	>175	29	>50	0.002	19, 15, 36
$NHCH_3$	**11**	0.007±0.002 (6)	0.33±0.24 (6)	0.44±0.17 (3)	-5.3	>175	>30	>50	0.008	<15, 28, <15
N	**12**	0.009±0.007 (32)	0.16±0.56 (48)	0.71±0.69 (24)	-4.6	>175	>30	>50	0.032	34, 33, 36
HN	**13**	0.004±0.001 (6)	0.071±0.11 (27)	0.55±0.34 (12)	-4.2	>175	25	28	0.037	52, 77, 28
HN O	**14**	0.03±0.06 (27)	0.18±0.14 (42)	0.97±1.7 (30)	-4.5	>175	>30	33	0.009	57, 60, 67
HN S O O	**15**	0.008±0.007 (6)	>10 (15)	>10 (12)	-4.8	120	>30	>50	0.021	107, ND, 78
HN O	**16**	0.004±0.002 (6)	>10 (12)	5.2±4.5 (12)	-4.6	>175	>30	24	0.022	63, ND, 45
HN O	**17**	0.01±0.004 (8)	0.05±0.04 (21)	0.35±0.16 (9)	-4.8	>175	22	ND	ND	27, <15, <15
N	**18**	0.005±0.005 (15)	0.12±0.03 (12)	0.53±0.82 (6)	-4.7	ND	>30	>50	0.015	96, 65, 30
N	**19**	0.003±0.004 (106)	0.085±0.12 (160)	0.35±0.57 (108)	-4.7	>175	11	18	0.022	62, 24,55
N O	**20**	0.004±0.003 (6)	0.03±0.03 (33)	2.1±2.1 (6)	-4.1	>175	>30	>50	0.038	130, 246, 175
N O	**21**	0.01±0.02 (18)	0.02±0.03 (18)	1.5±1.1 (18)	-3.9	>175	>30	>50	0.031	130, 440, 55
HN F F	**22**	0.012±0.003 (6)	0.14±0.07 (12)	ND	-3.7	>175	>30	8.6	0.011	423, ND, 656

[a]Potency in cellular assays for TLR7, TLR8, and TLR9 (PBMCs) as described in the Supporting Information. IC_{50} in μM ± geomeans; numbers in brackets denote number of independent experiments. HT solubility and CYP3A4 inhibition (μM), TDI: Kobs (min^{-1}), hERG: ^{3}H-dofetilite displacement assay (μM). Metabolic clearance: CL_{int} (μL/min/mg). ND = not determined.

Scheme 3. Synthetic Route for Compounds 23−30[a]

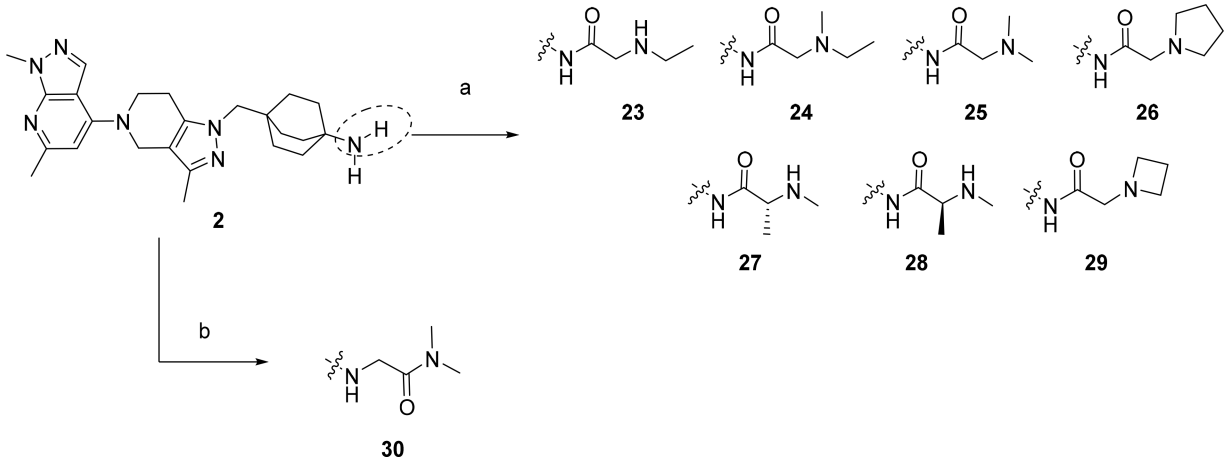

[a]Reagents and conditions: a. Corresponding amino acid (boc-protected where required), HATU, DIEPA, DCM, RT, then HCl-dioxane. b. (**30**) 2-bromo-*N*,*N*-dimethylacetamide, Cs_2CO_3, DMF, RT.

https://doi.org/10.1021/acsmedchemlett.3c00136
ACS Med. Chem. Lett. 2023, 14, 1054−1062

Scheme 4. Synthetic Route for Compounds 31−35[a]

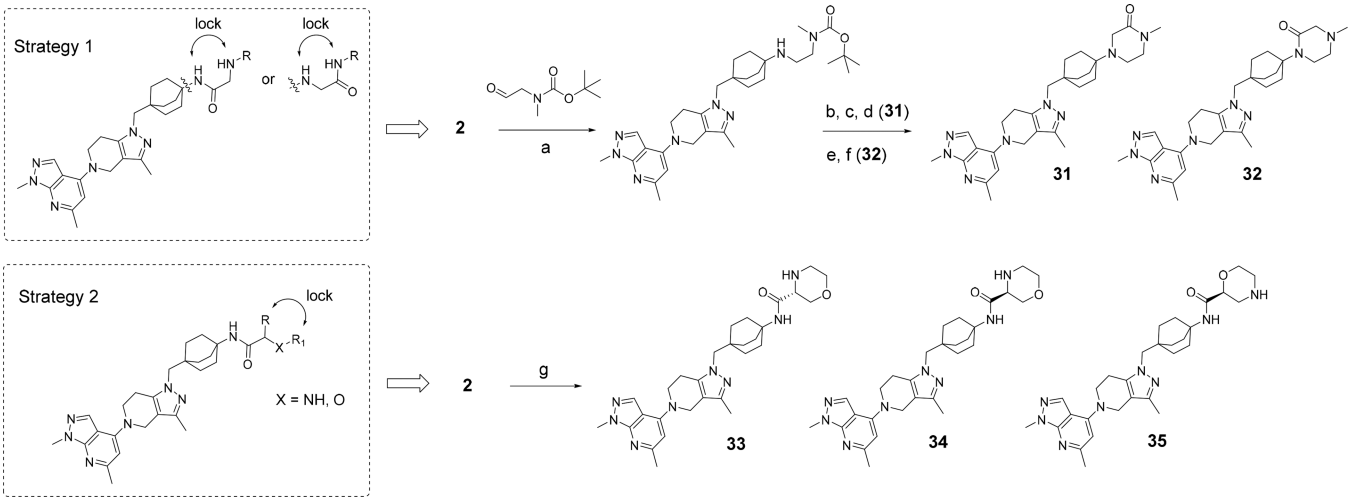

[a]Reagents and conditions: a. *tert*-Butyl methyl(2-oxoethyl)carbamate, $NaBH(OAc)_3$, CPME, RT. b. 2-Bromoacetate, K_2CO_3, EtOH, MW irradiation, 150°C, 1 h then 1 N NaOH, RT. c. HCl-dioxane, RT. d. HATU, DIEPA, DMF, 0 °C. e 2-Bromoacetylbromide, DIEPA, DCM, 0°C to RT followed by HCl-dioxane, RT. f. K_2CO_3, EtOH, MW irradiation, 120 °C, 40 min followed 1 N aqueous HCl and lyophilization. g. Corresponding morpholino carboxylic acid, HATU, DIEPA, DCM, RT, then HCl-dioxane.

(mostly mono- and disubstituted alkyl and heteroalkyl derivatives). Scheme 2 depicts a sample of the first round of SAR. The monomethyl amine derivative **11** was synthesized by condensation of **10** on **8** using Pd_2dba_3, Cs_2CO_3, RuPhos in dioxane at reflux, followed by boc deprotection (4 N HCl in dioxane at RT). Compounds **12**−**14** were synthesized by reductive amination of **2** using formaldehyde, cyclobutanone, and oxetan-3-one, respectively. Sulfonylation (DIPEA, $MeSO_2Cl$, DCM, 0 °C to RT) or acylation (DIPEA, AcCl, DCM, RT) of **2** afforded the corresponding sulfonamide **15** and acetamide **16**. A simple alkylation reaction (K_2CO_3, EtOH, 2-methoxyethyl bromide, 1,4-dibromobutane, 1-bromo-2-(2-bromoethoxy)ethane, 1,3-dibromopropane, and (*S*)-1-bromo-2-(((*R*)-1-bromopropan-2-yl)oxy)propane) was used to synthesize compounds **17**−**21**, respectively. Compound **22** was synthesized by condensation of 2,2-difluoroethyl trifluoromethanesulfonate in the presence of DIPEA in refluxing THF overnight.

Table 2 summarizes the findings associated with our first round of SAR using various amine-capping groups.

As predicted, most substitutions had a positive effect on permeability as measured using the PAMPA assay (Caco-2 followed a similar trend), and this first round of SAR provided interesting results. Alkyl, heteroalkyl and fluoroalkyl substituents (compounds **11**−**14** and **17**−**22**) were well tolerated to maintain potent TLR7/8 inhibition and improved their permeability. However, most compounds exhibited high human metabolic clearance in vitro (**14**−**16**, **18**−**22**) and this trend was consistent across most compounds synthesized. Time-dependent inhibition of CYP3A4 enzyme (as measured by high throughput time dependent enzymatic activity assay) also appeared to be high for some compounds (**12**, **13**, **15**, **16**, **18**−**22**). Surprisingly, the sulfonamide **15** and the carboxamide **16** displayed an excellent TLR7 inhibition profile (0.008 ± 0.007 and 0.004 ± 0.002 μM, respectively) but were inactive toward inhibition of TLR8 responses (>10 μM and 5.2 ± 4.5 μM, respectively). We hypothesized that TLR7/8 dual inhibition required a higher basicity than TLR7 inhibition and that therefore introducing an amine at a proximal distance to the amide would be a good strategy to maintain dual potency. To achieve this, we introduced simple capping groups like substituted glycine or alanine derivatives (resulting in **23**−**29**) or alkylamines possessing an alpha carboxamide (resulting in **30**) (Scheme 3). In our derivatization efforts, we used only a set of small amino acids to keep the molecular weight/PSA and cLogP under control. In parallel, we also tried to move the amide away from the octabicyclic amine moiety (only one example is shown, compound **30**) and found that these derivatives retained activity. Piperazinone (compounds **31**−**32**) and morpholinamide substituents in the octabicyclo system (compounds **33**−**35**) (Scheme 4) also retained activity.

The cellular potency on the TLR pathways and the properties for compounds **23**−**35** are shown in Table 3. In general, all compounds were potent TLR7 antagonists (IC_{50} < 0.07 μM). However, only a few derivatives showed sufficient TLR8 inhibition (**27**, **28**, **31**, and **36**). TLR9 pathway inhibition was generally weak across the series, as previously described.[9] Compounds **23**−**35** all showed good solubility (>175 μM). While most compounds had acceptable CYP inhibition profiles (CYP2D6, CYP3A1 comparable to CYP3A4, data not shown), one liability of this series was unpredictable human clearance in liver microsomes (**25**−**30** and **31**−**33**). Compound **30** had an interesting overall profile but showed time dependent CYP inhibition. Several derivatives were selected for PK profiling in parallel to evaluate *in vitro-in vivo* correlations. The mouse and rat PK profiles of compounds **23**, **28**, and **34** are illustrated in Table 4.

Of all these derivatives, the PK profile of compound **34** was most attractive. Compound **34** possessed adequate PK properties in mouse and rat, as it showed moderate clearance (11 and 18 $mL.min^{-1}.kg^{-1}$ respectively) and low Vss (0.7 and 1.3 L kg^{-1} respectively). The relatively short mean residence time (MRT) of 1 and 1.2 h, respectively, as well as moderate bioavailability (%F: 32 and 52 respectively) were considered sufficient for translation into acceptable parameters in human. It is notable that while the PAMPA score of **34** was similar to **2**, the Caco2 assay (ratio A-B/B-A = 1.92) was vastly superior, and this was reflected in better exposure.

https://doi.org/10.1021/acsmedchemlett.3c00136
ACS Med. Chem. Lett. 2023, 14, 1054−1062

Table 3. Profiling Data of Compounds[a]

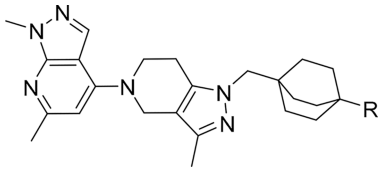

R		hTLR7	hTLR8	hTLR9	Log PAMPA	CYP3A4	TDI	hERG	Met Cl. (h, m, r)
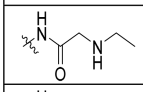	**23**	0.017±0.29 (15)	0.044±0.089 (18)	0.81±0.65 (14)	-5.3	>50	0.01	>30	35,96,<15
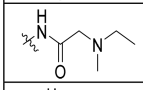	**24**	<0.005 (3)	0.007±002 (6)	0.26±0.09 (3)	-4.1	28	0.013	>30	463, >700, 48
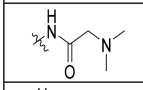	**25**	0.006±0.005 (93)	0.025±0.046 (92)	0.73±1.3 (78)	-4.3	>50	0.006	>30	147, 104, 33
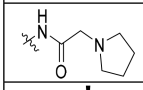	**26**	0.004±0.004 (9)	0.015±0.003 (6)	1.2±2.0 (6)	-4.1	ND	ND	ND	329, 531, <15
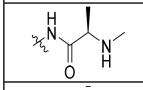	**27**	0.002±0.0008 (4)	0.19±0.09 (6)	0.78±0.57 (6)	-5.3	>50	0.023	>30	<15, 120, <15
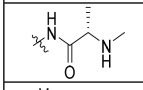	**28**	0.002±0.0007 (6)	0.19±0.05 (6)	0.70±1.3 (6)	-5.3	>50	0.022	>30	<15, 42, 34
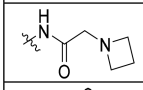	**29**	0.0009±0.00006 (3)	0.06±0.003 (2)	0.28±0.04 (4)	-4.6	17	0.044	>30	90, ND, 37
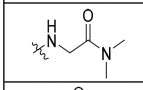	**30**	0.041±0.029 (9)	0.19±0.16 (21)	3.0±2.5 (9)	-5.4	ND	ND	ND	31, <15, 29
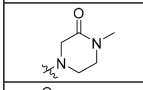	**31**	0.056±0.018 (6)	0.40±0.06 (6)	>7.3 (6)	-5.0	>50	0.015	>30	39, 103, 87
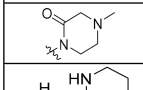	**32**	0.019±0.003 (3)	0.044±0.028 (6)	5.5±2.4 (12)	-4.3	>50	ND	>30	71, 251, 50
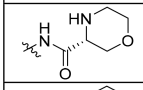	**33**	0.013±0.009 (11)	0.22±0.09 (14)	1.9±2.2 (12)	-5.3	>50	0.018	>30	54, 382, <15
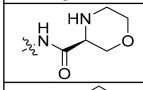	**34**	0.004±0.002 (39)	0.068±0.032 (16)	1.0±0.77 (20)	-5.2	>50	0.006	>30	49, 52, 17
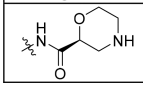	**35**	0.002±0.0006 (2)	0.067±0.010 (2)	0.190.07 (3)	-5.2	5.5	ND	ND	135, 93, 24

[a]Potency (IC_{50} in μM) within cellular assays for TLR7, TLR8, and TLR9 (PBMCs) as described in the Supporting Information. HT solubility and CYP3A4 inhibition (μM), TDI: Kobs (min^{-1}), hERG: ^{3}H-dofetilite displacement assay (μM). Metabolic clearance: CL_{int} (μL/min/mg). ND = not determined.

Table 4. Mouse and Rat PK Profiles of Compounds 23, 28, and 34[a]

	23		28		34	
	mouse	rat	mouse	rat	mouse	rat
CL ($mL \cdot min^{-1} \cdot kg^{-1}$)	7	19	37	19	11	18
Vss (L kg^{-1})	1	3	3.5	2	0.7	1.3
IV AUC (nM·h)	9276	1782	1790	1784	5672	1776
MRT (h)	2.4	2.8	1.6	1.6	1	1.2
PO C_{max} (nM)	515	48	237	31	1858	282
PO AUC (nM·h)	4629	618	2336	483	9160	2817
%F	10	12	26	9	32	52

[a]Formulation for IV and PO: 1 mg/mL in PEG300/D5W, 3:1; solution.

Compound **34** (MHV370) was profiled for inhibition of TLR7 and TLR8 responses and selectivity against TLR4 and TLR9 pathway activation in human PBMCs and whole blood. Compound **34** (MHV370) showed a slightly higher potency on TLR7 compared to TLR8 in both assay matrices (Table 5). In contrast, compound **34** (MHV370) showed very weak inhibition of TLR9 and was inactive against TLR4 (Table 5). Furthermore, compound **34** (MHV370) inhibited murine TLR7, yet it did not inhibit mouse TLR4 or TLR9, as shown on mouse splenocytes. In the preparation of *in vivo* experiments in mice, we also demonstrated potent and selective TLR7 inhibition in murine whole blood (Table 5). It was not possible to study TLR8 responses in murine assays, as rodent TLR8 does not recognize ssRNA ligands.[16] In

https://doi.org/10.1021/acsmedchemlett.3c00136
ACS Med. Chem. Lett. 2023, 14, 1054−1062

Table 5. Cellular Profile of Compound 34 (MHV370) on the Indicated TLRs[a]

	TLR7 (IFNα)	TLR8 (IL-6)	TLR9 (IFNα)	TLR4 (IL-6)
hPBMC	0.004 ± 0.002 (39)	0.068 ± 0.032 (16)	1.0 ± 0.77 (20)	>10 (10)
huWB	0.007 ± 0.004 (16)	0.074 ± 0.047 (4)	1.2 ± 0.52 (12)	>10 (4)
msSpleno	0.009 ± 0.003 (6)	NA	>1 (6)	>10 (4)
mWB	0.051 ± 0.027 (7)	NA	>10 (4)	>10 (4)

[a]Assay conditions are described in the Supporting Information. Geometric means of IC_{50} (μM) ± SD, number of individual experiments, or donors are indicated in parentheses. NA = Not applicable since mouse TLR8 does not recognize ssRNA ligands.

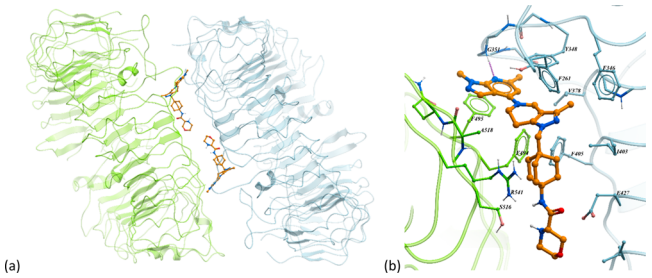

Figure 3. Cocrystal structure of compound 34 (MHV370) with TLR8 (PDB 8PFI). (a) Full view of the homodimeric structure and the two symmetrical binding sites formed between thae two TLR8 chains (one TLR8 monomer in light green and the second monomer in light blue), carbon atoms of compound **34** (MHV370) in orange. (b) Close-up view of one binding site showing amino acids in close contact with compound **34** (MHV370). Notable interactions include a hydrogen bond interaction (represented magenta dotted line) between the pyrazolo-pyridine moiety and Gly351 and many hydrophobic interactions between the central part of compound **34** (MHV370) and residues Phe261, Phe346, Val378, Ile403, Phe405, and Phe495.

addition, compound **34** (MHV370) showed high selectivity against other TLRs (Hawtin et al., under revision) and did not show any inhibition of catalytic activity on 46 kinases in a biochemical assay panel (assay details in the Supporting Information).

An X-ray cocrystal structure of compound **34** (MHV370) with the endosomal domain of human TLR8 confirmed their direct interaction (Figure 3). Similar to published structures (Tanji, Science2013) two TLR8 protomers build a homodimeric complex with an axial symmetry, forming at their interface two symmetrical binding pockets. A key interaction is the hydrogen bond between the pyrazolo-pyridine of compound **34** (MHV370) and the NH of Gly351. In addition, the central part of compound **34** (MHV370) is embedded in the hydrophobic pocket formed by the aromatic and aliphatic side chains of the two TLR8 moieties.

Based on the above data as well as superior PK and CYP inhibition profiles relative to **35**, we evaluated compound **34** (MHV370) *in vivo* in an acute PK/PD model. Oral dosing of MHV370 showed a dose-dependent suppression of IFNα, IL-6 and TNF in mice following challenge with the TLR7 ligand ssRNA/DOTAP. Near-complete inhibition of IFNα, IL-6, and TNF in plasma was observed with 10 mg/kg of compound **34** (MHV370) at 2 h post challenge (Figure 4).

These results encouraged us to further characterize **34** (MHV370) in more complex, chronic *in vivo* mouse models.[17] The safety and efficacy profiles in these studies were excellent, and thus a clinical trial has been initiated for MHV370 in patients suffering from Sjögren's syndrome (SjS) and mixed connective tissue disease (MCTD, NCT04988087). Two other TLR7/8 antagonists are in clinical development,

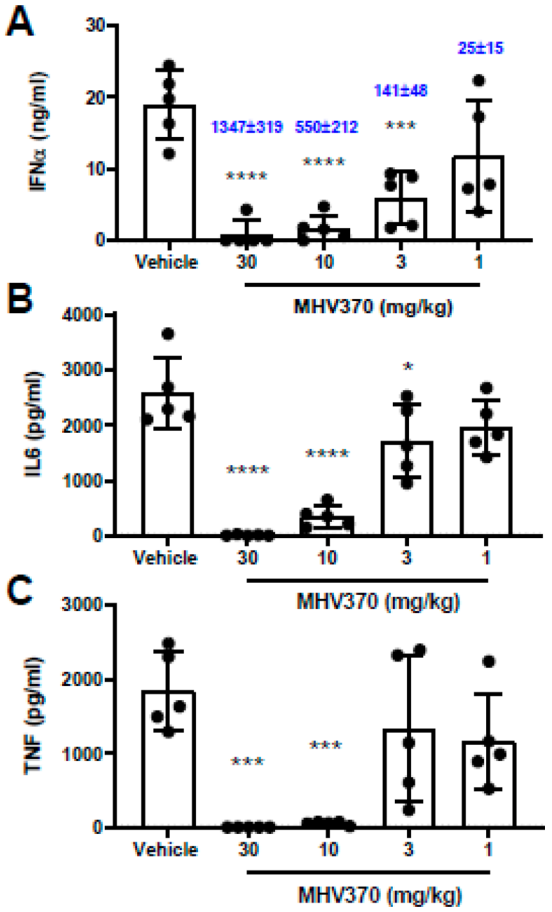

Figure 4. *In vivo* efficacy of compound **34** (MHV370). Compound **34** (MHV370) suppresses serum levels of multiple proinflammatory cytokines in mice after an acute TLR7 challenge. Bars represent means and SD, dots represent individual mice. Blue numbers represent blood exposures in nM (±SD), ***p > 0.001, ****p > 0.0001, ANOVA with Dunnett's post test.

afimetoran/BMS-986256 by BMS and enpatoran/M5049 by Merck, and the *in vitro* and *in vivo* profile of enpatoran has been published.[18] Both enpatoran and MHV370 show a higher potency on TLR7 than on TLR8, and MHV370 shows a higher potency on TLR8 than that reported for enpatoran. Both compounds were only weakly active or inactive on TLR9 and both can be safely dosed in mouse models of chronic inflammation.[17,18]

In conclusion, a SAR campaign on compound **2** led to substitution of the amine present on **2** in order to address its deficiencies (weak potency and poor permeability, leading to poor oral exposure). Systematic SAR on that amide led to the identification of compound **34** (MHV370; (*S*)-*N*-(4-((5-(1,6-dimethyl-1*H*-pyrazolo[3,4-*b*]pyridin-4-yl)-3-methyl-4,5,6,7-tetrahydro-1*H*-pyrazolo[4,3-*c*]pyridin-1-yl)methyl)bicyclo[2.2.2]-

https://doi.org/10.1021/acsmedchemlett.3c00136
ACS Med. Chem. Lett. 2023, 14, 1054−1062

octan-1-yl)morpholine-3-carboxamide) which possesses a favorable balance of potency/PK and physicochemical properties. In the meantime, a Phase 2 clinical proof of concept study has been initiated for compound **34** (MHV370) for systemic autoimmune diseases with high unmet medical need [NCT04988087].

■ ASSOCIATED CONTENT

Supporting Information

The Supporting Information is available free of charge at https://pubs.acs.org/doi/10.1021/acsmedchemlett.3c00136.

Synthesis procedures and analytical data for compounds **1**−**2** and **11**−**35**; assay procedures; crystallographic information (the X-ray cocrystal structure of TLR8 ECD in complex with compound **34** (MHV370) is available in the PDB under the code 8PFI) (PDF)

■ AUTHOR INFORMATION

Corresponding Author

Phil Alper − *Novartis Institutes for Biomedical Research, San Diego, California 92121, United States;* orcid.org/0000-0002-4115-0633; Email: phillip.alper@novartis.com

Authors

Claudia Betschart − *Novartis Institutes for Biomedical Research, CH-4056 Basel, Switzerland;* orcid.org/0000-0002-7770-6605

Cédric André − *Novartis Institutes for Biomedical Research, CH-4056 Basel, Switzerland*

Thomas Boulay − *Novartis Institutes for Biomedical Research, CH-4056 Basel, Switzerland*

Dai Cheng − *Novartis Institutes for Biomedical Research, San Diego, California 92121, United States*

Jonathan Deane − *Novartis Institutes for Biomedical Research, San Diego, California 92121, United States;* Present Address: Kumquat Biosciences, 10770 Wateridge Circle, Ste. 120, San Diego, CA 92121, USA

Michael Faller − *Novartis Institutes for Biomedical Research, CH-4056 Basel, Switzerland*

Roland Feifel − *Novartis Institutes for Biomedical Research, CH-4056 Basel, Switzerland*

Ralf Glatthar − *Novartis Institutes for Biomedical Research, CH-4056 Basel, Switzerland*

Dong Han − *Novartis Institutes for Biomedical Research, San Diego, California 92121, United States*

Rene Hemmig − *Novartis Institutes for Biomedical Research, CH-4056 Basel, Switzerland*

Tao Jiang − *Novartis Institutes for Biomedical Research, San Diego, California 92121, United States*

Thomas Knoepfel − *Novartis Institutes for Biomedical Research, CH-4056 Basel, Switzerland;* orcid.org/0000-0002-1675-6297

Jillian Maginnis − *Novartis Institutes for Biomedical Research, San Diego, California 92121, United States*

Daniel Mutnick − *Novartis Institutes for Biomedical Research, San Diego, California 92121, United States*

Wei Pei − *Novartis Institutes for Biomedical Research, San Diego, California 92121, United States*

Giulia Ruzzante − *Novartis Institutes for Biomedical Research, CH-4056 Basel, Switzerland*

Peter Syka − *Novartis Institutes for Biomedical Research, San Diego, California 92121, United States*

Guobao Zhang − *Novartis Institutes for Biomedical Research, San Diego, California 92121, United States*

Yi Zhang − *Novartis Institutes for Biomedical Research, San Diego, California 92121, United States*

Florence Zink − *Novartis Institutes for Biomedical Research, CH-4056 Basel, Switzerland*

Géraldine Zipfel − *Novartis Institutes for Biomedical Research, CH-4056 Basel, Switzerland*

Stuart Hawtin − *Novartis Institutes for Biomedical Research, CH-4056 Basel, Switzerland*

Tobias Junt − *Novartis Institutes for Biomedical Research, CH-4056 Basel, Switzerland*

Pierre-Yves Michellys − *Novartis Institutes for Biomedical Research, San Diego, California 92121, United States;* Present Address: Odyssey Therapeutics, 4242 Campus Point Court, San Diego, CA 92121, USA

Complete contact information is available at: https://pubs.acs.org/10.1021/acsmedchemlett.3c00136

Author Contributions

PM, PA, JD, ToJu, and SH designed experiments and wrote the manuscript. CA, TB, GR, GZ, DC, DH, TaJa, JM, DM, WP, PS, GZ, and YZ conducted experiments. CB supported manuscript writing.

Notes

The authors declare no competing financial interest.

■ REFERENCES

(1) Kawai, T.; Akira, S. The role of pattern-recognition receptors in innate immunity: update on Toll-like receptors. *Nature immunology* **2010**, *11* (5), 373−84.

(2) Marshak-Rothstein, A.; Rifkin, I. R. Immunologically active autoantigens: the role of toll-like receptors in the development of chronic inflammatory disease. *Annual review of immunology* **2007**, *25*, 419−41.

(3) Junt, T.; Barchet, W. Translating nucleic acid-sensing pathways into therapies. *Nature reviews. Immunology* **2015**, *15* (9), 529−44.

(4) Brown, G. J.; Canete, P. F.; Wang, H.; Medhavy, A.; Bones, J.; Roco, J. A.; He, Y.; Qin, Y.; Cappello, J.; Ellyard, J. I.; Bassett, K.; Shen, Q.; Burgio, G.; Zhang, Y.; Turnbull, C.; Meng, X.; Wu, P.; Cho, E.; Miosge, L. A.; Andrews, T. D.; Field, M. A.; Tvorogov, D.; Lopez, A. F.; Babon, J. J.; Lopez, C. A.; Gonzalez-Murillo, A.; Garulo, D. C.; Pascual, V.; Levy, T.; Mallack, E. J.; Calame, D. G.; Lotze, T.; Lupski, J. R.; Ding, H.; Ullah, T. R.; Walters, G. D.; Koina, M. E.; Cook, M. C.; Shen, N.; de Lucas Collantes, C.; Corry, B.; Gantier, M. P.; Athanasopoulos, V.; Vinuesa, C. G. TLR7 gain-of-function genetic variation causes human lupus. *Nature* **2022**, *605* (7909), 349−356.

(5) Deane, J. A.; Pisitkun, P.; Barrett, R. S.; Feigenbaum, L.; Town, T.; Ward, J. M.; Flavell, R. A.; Bolland, S. Control of toll-like receptor 7 expression is essential to restrict autoimmunity and dendritic cell proliferation. *Immunity* **2007**, *27* (5), 801−10.

(6) Guiducci, C.; Gong, M.; Cepika, A. M.; Xu, Z.; Tripodo, C.; Bennett, L.; Crain, C.; Quartier, P.; Cush, J. J.; Pascual, V.; Coffman, R. L.; Barrat, F. J. RNA recognition by human TLR8 can lead to autoimmune inflammation. *Journal of experimental medicine* **2013**, *210* (13), 2903−19.

(7) Barrat, F. J.; Meeker, T.; Gregorio, J.; Chan, J. H.; Uematsu, S.; Akira, S.; Chang, B.; Duramad, O.; Coffman, R. L. Nucleic acids of mammalian origin can act as endogenous ligands for Toll-like receptors and may promote systemic lupus erythematosus. *Journal of experimental medicine* **2005**, *202* (8), 1131−9.

(8) Rodero, M. P.; Decalf, J.; Bondet, V.; Hunt, D.; Rice, G. I.; Werneke, S.; McGlasson, S. L.; Alyanakian, M. A.; Bader-Meunier, B.; Barnerias, C.; Bellon, N.; Belot, A.; Bodemer, C.; Briggs, T. A.; Desguerre, I.; Fremond, M. L.; Hully, M.; van den Maagdenberg, A.; Melki, I.; Meyts, I.; Musset, L.; Pelzer, N.; Quartier, P.; Terwindt, G.

M.; Wardlaw, J.; Wiseman, S.; Rieux-Laucat, F.; Rose, Y.; Neven, B.; Hertel, C.; Hayday, A.; Albert, M. L.; Rozenberg, F.; Crow, Y. J.; Duffy, D. Detection of interferon alpha protein reveals differential levels and cellular sources in disease. *Journal of experimental medicine* **2017**, *214*, 1547.

(9) Banchereau, R.; Hong, S.; Cantarel, B.; Baldwin, N.; Baisch, J.; Edens, M.; Cepika, A. M.; Acs, P.; Turner, J.; Anguiano, E.; Vinod, P.; Kahn, S.; Obermoser, G.; Blankenship, D.; Wakeland, E.; Nassi, L.; Gotte, A.; Punaro, M.; Liu, Y. J.; Banchereau, J.; Rossello-Urgell, J.; Wright, T.; Pascual, V. Personalized Immunomonitoring Uncovers Molecular Networks that Stratify Lupus Patients. *Cell* **2016**, *165* (3), 551.

(10) Herster, F.; Bittner, Z.; Archer, N. K.; Dickhofer, S.; Eisel, D.; Eigenbrod, T.; Knorpp, T.; Schneiderhan-Marra, N.; Loffler, M. W.; Kalbacher, H.; Vierbuchen, T.; Heine, H.; Miller, L. S.; Hartl, D.; Freund, L.; Schakel, K.; Heister, M.; Ghoreschi, K.; Weber, A. N. R. Neutrophil extracellular trap-associated RNA and LL37 enable self-amplifying inflammation in psoriasis. *Nat. Commun.* **2020**, *11* (1), 105.

(11) Avalos, A. M.; Busconi, L.; Marshak-Rothstein, A. Regulation of autoreactive B cell responses to endogenous TLR ligands. *Autoimmunity* **2010**, *43* (1), 76−83.

(12) Ganguly, D.; Chamilos, G.; Lande, R.; Gregorio, J.; Meller, S.; Facchinetti, V.; Homey, B.; Barrat, F. J.; Zal, T.; Gilliet, M. Self-RNA-antimicrobial peptide complexes activate human dendritic cells through TLR7 and TLR8. *Journal of experimental medicine* **2009**, *206* (9), 1983−94.

(13) Alper, P. B.; Deane, J.; Betschart, C.; Buffet, D.; Collignon Zipfel, G.; Gordon, P.; Hampton, J.; Hawtin, S.; Ibanez, M.; Jiang, T.; Junt, T.; Knoepfel, T.; Liu, B.; Maginnis, J.; McKeever, U.; Michellys, P. Y.; Mutnick, D.; Nayak, B.; Niwa, S.; Richmond, W.; Rush, J. S.; Syka, P.; Zhang, Y.; Zhu, X. Discovery of potent, orally bioavailable in vivo efficacious antagonists of the TLR7/8 pathway. *Bioorg. Med. Chem. Lett.* **2020**, *30* (17), 127366.

(14) Knoepfel, T.; Nimsgern, P.; Jacquier, S.; Bourrel, M.; Vangrevelinghe, E.; Glatthar, R.; Behnke, D.; Alper, P. B.; Michellys, P. Y.; Deane, J.; Junt, T.; Zipfel, G.; Limonta, S.; Hawtin, S.; Andre, C.; Boulay, T.; Loetscher, P.; Faller, M.; Blank, J.; Feifel, R.; Betschart, C. Target-Based Identification and Optimization of 5-Indazol-5-yl Pyridones as Toll-like Receptor 7 and 8 Antagonists Using a Biochemical TLR8 Antagonist Competition Assay. *Journal of medicinal chemistry* **2020**, *63* (15), 8276−8295.

(15) Vlach, J.; Bender, A. T.; Przetak, M.; Pereira, A.; Deshpande, A.; Johnson, T. L.; Reissig, S.; Tzvetkov, E.; Musil, D.; Morse, N. T.; Haselmayer, P.; Zimmerli, S. C.; Okitsu, S. L.; Walsky, R. L.; Sherer, B. Discovery of M5049: A Novel Selective Toll-Like Receptor 7/8 Inhibitor for Treatment of Autoimmunity. *J. Pharmacol Exp Ther* **2021**, *376* (3), 397−409.

(16) Forsbach, A.; Nemorin, J. G.; Montino, C.; Muller, C.; Samulowitz, U.; Vicari, A. P.; Jurk, M.; Mutwiri, G. K.; Krieg, A. M.; Lipford, G. B.; Vollmer, J. Identification of RNA sequence motifs stimulating sequence-specific TLR8-dependent immune responses. *J.Immunol.* **2008**, *180* (6), 3729−3738.

(17) Hawtin, S.; André, C.; Collignon-Zipfel, G.; Appenzeller, S.; Bannert, B.; Baumgartner, L.; Beck, D.; Betschart, C.; Boulay, T.; Brunner, H. I.; Ceci, M.; Deane, J.; Feifel, R.; Ferrero, E.; Kyburz, D.; Lafossas, F.; Loetscher, P.; Merz-Stoeckle, C.; Michellys, P.; Nuesslein-Hildesheim, B.; Raulf, F.; Rush, J. S.; Ruzzante, G.; Stein, T.; Zaharevitz, S.; Wieczorek, G.; Siegel, R.; Gergely, P.; Shisha, T.; Junt, T. Preclinical characterization of the Toll-like receptor 7/8 antagonist MHV370 for lupus therapy. *Cell Rep. Med.* **2023**, *4*, 101036.

(18) Vlach, J.; Bender, A. T.; Przetak, M.; Pereira, A.; Deshpande, A.; Johnson, T. L.; Reissig, S.; Tzvetkov, E.; Musil, D.; Morse, N. T.; Haselmayer, P.; Zimmerli, S. C.; Okitsu, S. L.; Walsky, R. L.; Sherer, B. Discovery of M5049: A Novel Selective Toll-Like Receptor 7/8 Inhibitor for Treatment of Autoimmunity. *J. Pharmacol. Exp. Ther.* **2021**, *376* (3), 397−409.

https://doi.org/10.1021/acsmedchemlett.3c00136
ACS Med. Chem. Lett. 2023, 14, 1054−1062